OPERATING POINT OPTIMIZATION OF SELF-LINEARIZED DIFFERENTIAL QUANTUM WELL ELECTROABSORPTIVE MODULATOR

F. Yazdani[1] and E. A. De Souza[2]
[1] Núcleo de Engenharia Elétrica, Universidade Federal de Sergipe, Av. Marechal Rondon, s/n Jardim Rosa Elze, São Cristóvão-SE 49100-000, Brasil
[2] Universidade Presbiteriana Mackenzie, Laboratório de Fotônica, Rua da Consolação 896, São Paulo-SP 01302-907, Brasil; Corresponding author: thoroh@mackenzie.br

Received 31 March 2009

ABSTRACT: *Electroabsorptive modulators require large depth of modulation and maximum length of in–out linearity. A systematic approach to optimize the operation of these modulators based on quantum-confined Stark effect is presented here. The conventional operation of differential modulator, following span linearity maximization by adjusting the incident power of laser beams and modulation depth enhancement by reverse bias voltage adjustment, is presented. The results show the optimum bias voltage as 8 V and read out beam power as 175 nW.* © 2009 Wiley Periodicals, Inc. Microwave Opt Technol Lett 52: 1–4, 2010; Published online in Wiley InterScience (www.interscience.wiley.com). DOI 10.1002/mop.24815

Key words: *quantum well; differential modulator; quantum-confined stark effect*

1. INTRODUCTION

Electroabsorptive (EA) multiple quantum well modulators (MQWM) are important in optical signal processing such as real space image filtering [1–3]. The potential of AlGaAs/GaAs MQW pin diode technology and the speed of MQW modulators make them suitable for many electro-optical applications. Large array of MQWM are used vastly in optical information processing, such as optical correlators, optical image filters, laser beam control, and high frequency analog modulation [4–7].

Surface reflection modulators have a particular interest, providing a double length of interaction between the light and the material, improving the modulation contrast [8–10]. The modulating signal is the current supplying to the reverse bias modulator diode and the carrier is an illuminating beam of diode. A feedback is made by the current, absorbed power, and the voltage across the diode. Linear analog modulation is performed at band-edge wavelength of absorption, where the absorption enhances through higher voltage, giving rise to a negative feedback, known as self-linearized mode of operation [9, 10].

Span of linearity is enhanced using differential QWMs (see Fig. 1), making easy to work with bipolar modulating signal [9–13]. In addition, it eliminates the effect of carrier beam fluctuation, using a single carrier source.

The differential output power (P_{o2}–P_{o1}) is a linear function of modulating current i as:

$$P_{o2} - P_{o1} = P_{i2} - P_{i1} + \frac{\hbar w_i}{e} i \quad (1)$$

where P_{i1} and P_{i2}, are the incident power beams, P_{o1} and P_{o2} are the output beams reflected from the two quantum well modulators, $\hbar\omega_i$ is the energy of the incident photons, and e the electrical charge. Using equal sources of carrier, i.e., $P_{i1} = P_{i2}$:

$$P_{o2} - P_{o1} + \frac{\hbar w_i}{e} i. \quad (2)$$

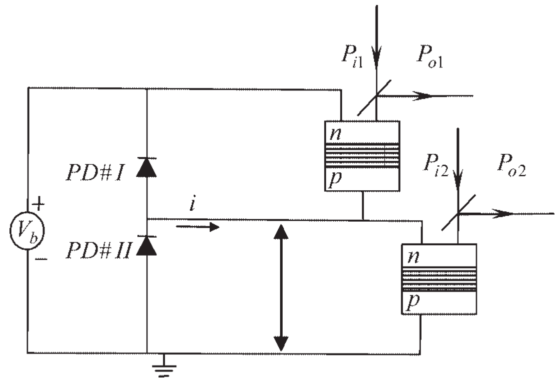

Figure 1 Self-linearized differential modulator circuits with two conventional photodiodes providing a current proportional to the input beams at 780 nm

Although, this equation shows the linear mode of carrier modulation, the effect of operating point is not so clear. In the literature, the applied voltage is adjusted at about 7 V without any notes about the power of carrier beams [12, 13].

In this paper, we verified the effect of reverse bias voltage and input power on the span of linearity and modulation depth. We showed that the bias voltage of about 8 V and carrier power of about 175 nW can optimize the operation. Also, we encountered a trade-off between the bias voltage and carrier power to operate in self-linearized mode. These arguments are explained in the following Sections, finalized by conclusion.

2. EXPERIMENTAL DETAIL

Multiple quantum well p-i-n diode has been grown by molecular beam epitaxy over an undoped dielectric mirror. The MQW region is ~1.2 μm thick consisting of 95 alternate thin layers of GaAs wells of 90 Å width, and 35 Å thickness barriers of $Al_{0.3}Ga_{0.7}As$ in intrinsic region. The fabrication process is discussed in Ref. [14]. The 95 periods of quantum wells in intrinsic region realizes to have the exciton peak at zero bias shorter than 850 nm wavelength. The current control element is a differential photodiode (PD). The area of MQW modulators and PDs are 7×7 and 10×10 μm^2, respectively. An antireflection coating has been used to avoid the resonator effects. The integrated configuration of diodes is reverse biased with 8 V in default. All the experiments were taken at room temperature.

3. OPERATION AT CONVENTIONAL OPERATING POINT

Linear operation of modulator can be verified through the differential output power measurement as a function of input control current. As the input current is supplied by the differential PDs, the linearity is verified through optical in–out considering the linear operation of PDs. The linearity of PDs is promised by the double size of PDs and the sufficient reverse bias. Positive polarity of current is supplied by illumination of PD #1 and negative one by illumination of PD #2. The result of measurements is shown in Figure 2.

As illustrated, the modulation is partially linear. The linearity span is in the order of the carrier input power due to equal quantum conversion efficiency in modulators and detectors. Beyond this value, the differential output was maintained approximately constant, i.e., it is saturated. It is due to the insufficient exciton generation by the incident carrier beams in comparison to net photocurrent generation of PDs. The span linearity can be extended applying more power of readout beams

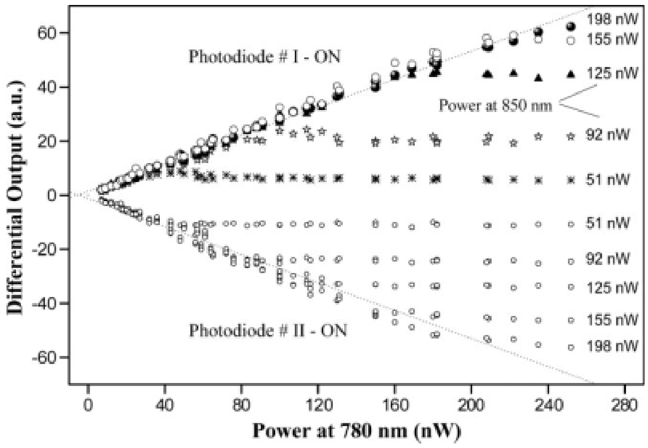

Figure 2 Differential output of modulator as a function of current (incident beam on PD #I or II considering the power of carrier beams as a parameter. Bias field of 6.7×10^4 V/cm

P_{850}, in which generates more excitons, supporting larger net photocurrent. Although the linear dynamic range varies as a function of readout beams, the modulation depth is constant, indicated by invariable gradient of the in–out curve, as predicted by Eq. (2). The improvement of span linearity is slowed-down at $P_{850} > 155$ nW due to sublinear increase of heavy hole (hh) photocurrent as a function of readout beam power and is terminated at $P_{850} = 198$ nW with a maximum extension of linearity of 235 nW (solid spheres). It can be explained by the exciton saturation, such that the high intensity of ionized excitons changes the dielectric constant, increasing the size of remaining excitons. Therefore, the optical absorption strength decreases [15, 16].

4. EFFECT OF REVERSE BIAS VOLTAGE

The optimized bias voltage was encountered fixing the readout beams (175 nW). For a given bias voltage, the differential output power is verified as a function of modulating current (PD ''I'' on) as illustrated in Figure 3. Low bias voltage such as 1 V is not sufficient to extend the depletion layer to the intrinsic region of MQW PDs, such that the probability of recombination of photocarrier is high. The reduced recombination time (carrier lifetime) gives rise to small quantum efficiency. Hence, the linear dynamic range of PDs are small, influencing the measurement of in–out characteristic of the modulator. On the other hand, the insufficient bias voltage increases insignificantly the exciton area. This gives origin to small reduction of exciton energy or insignificant shift of exciton resonance to the longer wavelength, although the density of exciton is high (generated by 175 nW incident beam). Hence, the quantum-confined stark effect (QCSE) is very small, which corresponds to an insignificant modulation depth. Also, the small quantum efficiency of quantum well modulators produce insignificant photocurrent, reduces the saturation level, and the linearity range of EAMs.

As can be seen in Figure 3, applying a bias voltage lager than 2 V enhances the linear dynamic range to maximum and increases the depth of modulation due to quantum efficiency elevation. This improvement of quantum efficiency of PDs is because of the extension of the depletion layer through the entire intrinsic region, such that almost all photocarriers are collected in the external contacts by the applied field. The sufficient applied field reduces the probability of photocarrier capture in the wells, enhancing the carrier lifetime and linear dynamic range of PDs. The same phenomenon occurs in MQW modulators giving rise to a quantum efficiency enhancement. Also, the high electric field increases the 2D-radius of the exciton corresponding to exciton energy reduction; hence the exciton frequency resonance is reduced giving rise to a considerable QCSE. The large red-shift of the absorption spectra enhances the contrast of the EA modulation.

The maximum depth of modulation and span of linearity is obtained at 10 V. More bias voltage such as 10.5 V enhances the area of the exciton, reduces the resonance frequency of the exciton, and reduces the strength of the exciton absorption. The large 2D-radius of exciton enhances the probability of exciton ionization [17, 18]. This phenomenon reduces the exciton lifetime, therefore deteriorates the EA effect. This case corresponds to the large stark shift, such that the exciton resonance moves to the longer wavelength than 850 nm. In this case, the differential MQW modulators do not operate anymore in self-linearized mode. The feedback is now positive, such that the optical absorption of MQW modulator is reduced by higher electric field [9–11]. This subject is explained in more details in the following section.

5. EFFECT OF REVERSE BIAS VOLTAGE AT LOW INTENSITY OF CARRIER

This experiment was performed at low intensity of readout beams (power at 850 nm was 51 nW) to show the effect of the power of readout beams on the optimized bias voltage (see Fig. 4). The comparison between Figures 3 and 4 show that at low bias voltage such as 1 V, the span and the modulation contrast are reduced considerably. The reduced span and modulation depth are due to reduced density of exciton produced by incident readout beams.

As explained before, the modulation depth and range of linearity are improved at higher bias voltage such as 2 V. This bias voltage is sufficient to extend the depletion layer to entire intrinsic region of PDs, maximizing the quantum efficiency. Therefore, the PDs work linearly. However, the insufficient density of excitons reduces the modulator range of linearity to 32 nW. Also, the bias voltage of 2 V is sufficient to obtain the maximum modulation depth that is nearly one order of magnitude less than the previous result. The linear dynamic range was improved to 65 nW at 3 V that is nearly the same as the incident power.

The device characteristic at 5 V showed a little improvement of modulation depth, but the range of linearity remained at 65

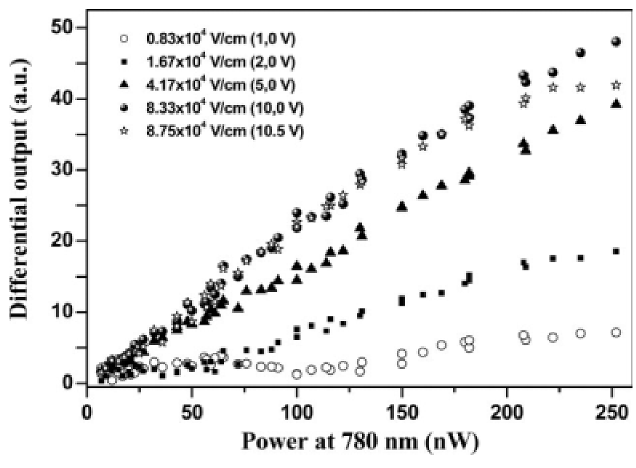

Figure 3 Differential output of modulators for PD #I ON, considering the bias fields as a parameter ($P_{850} = 175$ nW)

nW. A dip after the knee was observed for powers larger than 65 nW. After the knee, the differential output was reduced as a function of the incident power up to 107 nW. Then, it saturates such that the differential output remains fixed as a function of input. At higher input, the current into the modulators and the optical absorption is reduced indicating the exciton resonance shifts to wavelengths longer than 850 nm. It means that there is a change in the modulators of operation mode from self-linearized to bistable one [10]. The same behavior is observed at 8 V with a slight reduction of modulation depth. This effect is explained through the large red-shift of hh-exciton peak, such that the peak is shifted to wavelength longer than 850 nm at 8 V and the absorption strength of the exciton peak is reduced. From the above observations, the optimum bias voltage must be <5 V, demonstrating the trade-off between optimum incident power and optimum reverse bias.

6. CRITICAL VOLTAGE

The critical voltage is defined as a voltage that the self-linearized mode of operation (negative feedback) changes to bistable mode (positive feedback). At this voltage, the exciton peak is shifted to the longer wavelength than 850 nm such that the exciton strength is reduced. This voltage depends on the intensity of the incident beams, shifting to lower voltages at lower intensity of control beams. Figure 5 shows the differential output power as a function of the bias voltage where the power of readout beams are considered as a parameter, and the PD #1 was illuminated by a 252 nW beam. This incident power can produce sufficient control current for differential modulators.

The modulation depth was small at low voltages (optical power at 850 nm of 42 nW), and was improved a little at higher voltages. It is due to the insufficient exciton generation, giving rise to insignificant EA modulation. Therefore, the extension of the depletion layer does not help to enhance the modulation contrast. However, at higher incident power at 850 nm, such as 51, 59, and 68 nW, the enhancement of the modulation depth was observed. Up to $\sim$2 V, the elevation is due to quantum efficiency improvement of both the PD and the MQW modulators. The depletion region is extended entirely through the intrinsic region at $\sim$2 V. Hence, the quantum efficiency of the PD is saturated, it is possible to have more Stark shift through the QCSE for modulators.

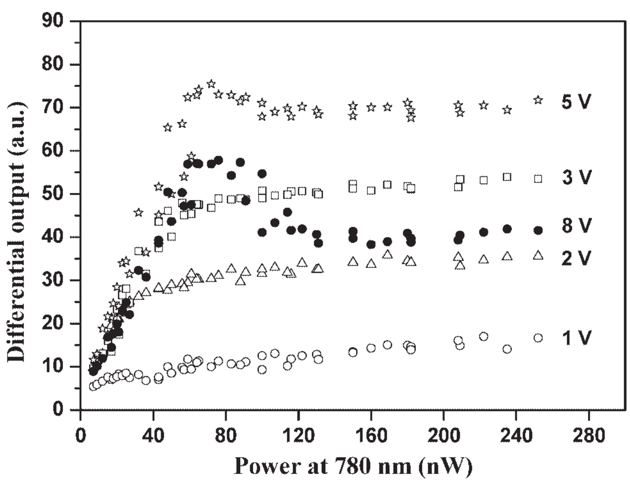

Figure 4 Differential output of modulators for PD #I ON, considering the bias fields as a parameter ($P_{850} = 51$ nW)

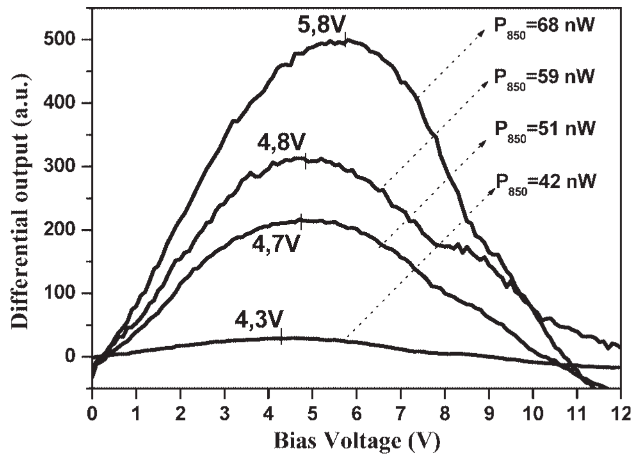

Figure 5 Differential output of modulators for PD #I ON as a function of bias voltage, considering the power of carrier beams as a parameter. Incident power on PD #I is 252 nW

The improvement reached to a critical voltage, such that more bias voltage gave rise to a reduction of differential output indicating a change in the mode of operation to bistable or positive feedback [10]. Therefore, the hh-exciton resonance is red-shifted to the longer wavelength than 850 nm. In Figure 5, the rising of the differential output as a function of incident light (power at 850 nm) indicates the modulation saturation corresponding to the modulation depth enhancement. The critical voltage rises as a function of incident light at 850 nm. It was enhanced from 4.3 V at 42 nW, to 5.8 V at 68 nW, and to 10.5 V at 175 nW. The increment of this voltage might be explained through nearly constant electric field strength per exciton density.

7. CONCLUSIONS

The monolithic EA device based on the AlGaAs/GaAs MQWs technology was presented. The differential modulator operating in analog self-linearized mode was optically and electrically biased. State of the diodes was read-out using a pair of beams in the bandtail. The linearity of operation was theoretically discussed and experimentally verified followed by the optimization of the operation. We observed the optimum bias voltage as 8 V, readout beam power as 175 nW, and the trade-off between optimum bias voltage and the intensity of incident readout beams.

ACKNOWLEDGMENTS

We thank CNPq for financial support and Prof. David A.B. Miller for supplying the samples.

REFERENCES

1. F. Yazdani and E. A. de Souza, Cross-differentiator image processor based on self-electrooptic effect, Electron Lett 43 (2007), pp 57–59.
2. J.F. Aquino and E.A. de Souza, Differential and direction-sensitive detector based on self-electro-optic effect in GaAs multiple quantum well, Electron Lett 41 (2005), pp 1350–1351.
3. C.J. Vianna, F. Yazdani, and E.A. de Souza, Characterisation of an analogue self-electro-optic effect device with five photodetectors as edge detector, Electron Lett 38 (2002), pp 119–121.
4. S. Junique, Q. Wang, S. Almqvist et al., GaAs-based multiple-quantum-well spatial light modulators fabricated by a wafer-scale process, Appl Opt 44 (2005), pp 1635–1641.

5. J.S. Ahearn, M.H. Weiler, S.B. Adams et al., Multiple quantum well (MQW) spatial light modulators (SLMs) for optical data processing and beam steering, Proc SPIE 4457 (2001), pp 43–53.
6. U. Arad, E. Redmard, M. Shamay et al., Development of a large high-performance 2-D array of GaAs–AlGaAs multiple quantum-well modulators, IEEE Photonics Technol Lett 15 (2003), pp 1531–1533.
7. G.L. Li and P.K.L. Yu, Optical intensity modulators for digital and analog applications, J. Lightwave technol 21 (2003), pp 2010–2030.
8. G.D. Boyd, D.A.B. Miller, D.S. Chemla et al., Multiple quantum well reflection modulator, Appl Phys Lett 50 (1987), pp 1119–1121.
9. D.A.B. Miller, Novel analog self-electro-optic effect devices, IEEE J Quantum Electron 29 (1993), pp 678–698.
10. D.A.B. Miller, D.S. Chemla et al., The quantum well self-electro-optic effect device: optoelectronic bistability and oscillation, and self-linearized modulation, IEEE J Quantum Electron QE-21 (1985), pp 1462–1476.
11. D.A.B. Miller, D.S. Chemla et al., Optical-level shifter and self-linearized optical modulator using a quantum-well self-electro-optic effect device, Optics Lett 9 (1984), pp 567–569.
12. E.A. De Souza,L. Carraresi, G.D. Boyd, and D.A.B Miller, Analog differential self-linearized quantum-well self-electro-optic-effect modulator, Optics Lett 18 (1993), pp 974–976.
13. E.A. De Souza, L. Carraresi, G.D. Boyd, and D.A.B. Miller, Self-linearized analog differential self-electrooptic-effect device, Appl Optics 33 (1994), pp 1492–1497.
14. L.M.F. Chirovsky, N.W. Focht, M. Freund et al., OSA Proceeding series, In: Photonic switching, Optical Society of America, Washington, DC, 8 (1991), pp 56.
15. A.M. Fox, D.A.B. Miller, G. Livescu et al., Exciton saturation in electrically biased quantum wells, Appl Phys Lett 57 (1990), pp 2315–2317.
16. G.D. Boyd, J.A. Cavailles, L.M.F. Chirovsky, D.A.B. Miller, Wavelength dependence of saturation and thermal effects in multiple quantum well modulators, Appl Phys Lett 63 (1993), pp 1715–1717.
17. D.A.B. Miller, Optical physics of quantum wells, In: G.-L. Oppo, S.M. Barnett, E. Riis, and M. Wilkinson (Eds.), Quantum dynamics of simple systems, Institute of Physics, London, 1996, pp 239–266.
18. D.A.B. Miller, J.S. Weiner, and D.S. Chemla, Electric field dependence of linear optical properties in quantum well structures: waveguide electroabsorption and sum rules, IEEE J Quantum Electron QE-22 (1986), pp1816–1830.

NOVEL MICROSTRIP BANDPASS FILTER BASED ON DEFECTED GROUND STRUCTURE AND SLOTLINE COUPLING TECHNIQUES

Wenjie Feng,[1] Kuan Deng,[1] Wenquan Che,[1] and Shiwei Dong[2]
[1] Department of Communication Engineering, Nanjing University of Science & Technology, 210094 Nanjing, China; Corresponding author: yeeren_che@yahoo.com.cn
[2] National Key Laboratory of Space Microwave Technology, Xi'an, China

Received 1 April 2009

ABSTRACT: *A novel microstrip bandpass filter integrating the defected ground structure and slotline coupling technique is presented in this letter. A slotline resonator with a length of three-quarter wavelength at central frequency is etched on the ground, while a pair of radial stubs is centrally introduced. Two microstrip open stubs are then placed above the slotline resonator, saying, on the top plane of the dielectric substrate. By properly adjusting the lengths of the microstrip stubs, a wideband passband filter is thus implemented using coupling between 50-Ω microstrip (on the top plane) and the slotline (on the bottom). A prototype is fabricated to validate the proposed design strategies. The experiments and simulations both indicate good performances. The measured fractional bandwidth of prototype is about 89%, the return loss is less than –15 dB in the whole passband. In addition, the measured rejection bandwidth at –25 dB is even higher up to 10 GHz, thus, demonstrating a very good harmonic suppression ability.* © 2009 Wiley Periodicals, Inc. Microwave Opt Technol Lett 52: 4–6, 2010; Published online in Wiley InterScience (www.interscience.wiley.com). DOI 10.1002/mop.24816

Key words: *microstrip bandpass filter; defected ground structure; slotline; radial stub; fractional bandwidth*

1. INTRODUCTION

To realize wideband bandpass filter (BPF), a strong coupling between the feed lines at the first- and last-stage resonators are required in the conventional uniplanar technology. Undoubtedly, broadside coupling structure is an efficient solution to solve this problem. Using such coupling technique, many advantages can be obtained, such as wide passband with low insertion loss, wide stopband with good rejection performance, etc. [1–5]. Microstrip transmission lines in combination with slotline [6–9] is a very typical solution to carry out broadside coupling [10], which can offer an additional freedom in the design of microwave integrated circuitry.

In this letter, one technique is employed to realize broadside coupling between 50-Ω microstrip and slotline, while a back-to-back transition is formed naturally. In addition, a pair of radial stubs is used to suppress the spurious harmonics and improve the impedance match. Two microstrip open stubs are then placed above the slotline resonator, saying, the top plane of the dielectric substrate, a wideband pass filter can thus be realized by properly folding the microstrip stubs. One prototype was fabricated to validate the proposed strategies, the simulated and measured results agree well with each other, both indicating that the filter has a fractional bandwidth (FBW) of 89% (1.7–4.4 GHz), the return loss is less than –15 dB in the whole passband; the out-of-band rejection at –25 dB is from 5 to 15 GHz, implying a very good potential to suppress the spurious harmonics.

2. DESIGN STRATEGIES OF THE PROPOSED BANDPASS FILTER

2.1. Determination of the Filter Structure

Figure 1(a) illustrates the geometry of the proposed novel BPF using microstrip–slotline coupling technique. The center frequency for the proposed filter $f_0 = 3$ GHz, which is constructed into the dielectric substrate with $\varepsilon_r = 2.65$ and a height of 0.508 mm. The microstrip width of 50-Ω input- and output-ports $W_1 = 1.4$ mm, two-folded microstrip open stubs with width $W_2 = 0.6$ mm are designed on the top plane of the dielectric substrate. A $(3/4)\lambda_g$ (λ_g is wavelength at central frequency) slotline resonator with a pair of radial stub at the center is etched on the ground. The length of the central section of the slotline: $L_3 = 11.4$ mm, $L_4 = 17.75$ mm, and $L_5 = 2.2$ mm. In this way, the total length of the slotline is 52.9 mm, almost equal to $(3/4)\lambda_g$ at the central frequency. Noting that, the 50-Ω microstrip and coupling slotline naturally form a back-to-back transition, which is a new and a simple technique to realize the broadside coupling. As we know, the center frequency of the passband is primarily determined by the length $L_1 + L_2$ ($L_1 = 10.4$ mm and $L_2 = 7.2$ mm) of the microstrip open stubs, which is nearly equal to $(1/4)\lambda_g$ at the central frequency. The distance of the two-folded microstrip open stubs is $d = 17$ mm, approximately a quarter wavelength at the central frequency.